Cement & Concrete Composites 32 (2010) 657–664

Contents lists available at ScienceDirect

Cement & Concrete Composites

journal homepage: www.elsevier.com/locate/cemconcomp

Stress–strain behaviour and abrupt loss of stiffness of geopolymer at elevated temperatures

Zhu Pan [a], Jay G. Sanjayan [b,*]

[a] Department of Civil Engineering, Monash University, Clayton, VIC 3800, Australia
[b] Faculty of Engineering and Industrial Sciences, PO Box 218, Hawthorn, VIC 3122, Australia

ARTICLE INFO

Article history:
Received 6 October 2009
Received in revised form 15 June 2010
Accepted 10 July 2010
Available online 15 July 2010

Keywords:
Geopolymer
Strength
Glass transition
Elevated temperatures
Fire
Stress versus strain
Hot strength

ABSTRACT

This paper reports stress versus strain curves of geopolymer tested while the specimens were kept at elevated temperatures, with the aim to study the fire resistance of geopolymer. Tests were performed at temperatures from 23 to 680 °C and after cooling. Hot strengths of geopolymer increased when the temperature increased from 290 to 520 °C, reaching the highest strength at 520 °C, which is almost double that of its initial strength at room temperature. However, glass transition behaviour was observed to occur between 520 and 575 °C, which was characterised by abrupt loss of stiffness and significant viscoelastic behaviour. The glass transition temperature is determined to be 560 °C. Further, the strength reductions occurred during cooling to room temperature. This is attributed to the damage due to brittle nature of the material making it difficult to accommodate thermal strain differentials during cooling phase.

1. Introduction

The term 'geopolymers' are generally applied to describe materials which are formed through hydrothermal synthesis of aluminosilicates in the presence of concentrated alkaline or alkaline silicate solution [1]. They have great potential to be used as building materials alternative to traditional Portland cement because strength, stiffness and other mechanical properties of geopolymers are comparable to Portland cement concretes. Further, geopolymers are produced from fly ash which is an industrial by-product, hence geopolymers are not responsible for large carbon footprint like Portland cement. Geopolymer concrete can be made by using low-calcium (ASTM Class F) fly ash [2–4]. Rangan et al. [2–4] reported that geopolymer concrete exhibited very little shrinkage and superior durability in sulphate environments. Besides the above advantages, another key benefit of geopolymers is their intrinsic fire resistance originating from their inorganic framework structure [5]. Due to this benefit, geopolymers are attracting increasing interest to be used as ecologically friendly fireproof building materials.

The previous studies [6–10] of geopolymers have been conducted to investigate their residual mechanical properties after exposure to elevated temperatures. Despite a number of publications suggesting the advantages of geopolymers in high temperature applications and showing evidences of their ability to have high residual strengths after exposure to 800 °C, the studies have not focused on their mechanical properties in the hot state. Behaviour of geopolymer at high temperatures while hot is important to assess the fire endurance of structures made with this material.

Therefore, the primary aim of the investigation was to experimentally study the mechanical properties of geopolymer at elevated temperatures. Since the material in a structure is normally in a stressed state, the effect of heating the specimen whilst under stress was also investigated. To provide data for estimating the strength of geopolymer after a fire, the effect of heating the specimens and testing when cooled was investigated as well. The physical evolutions, such as thermal deformation and weight loss of geopolymer, were also investigated and related to its changes in the mechanical properties.

2. Experimental program

2.1. Materials

Fly ash (ASTM Class F) was used as the main aluminium and silicate source for synthesising of geopolymeric binder. It is mainly glassy with some crystalline inclusions of mullite, hematite and quartz. The chemical composition of the fly ash used in this experimental program is shown in Table 1.

* Corresponding author. Tel.: +61 3 92148034; fax: +61 3 92148264.
E-mail address: jsanjayan@swin.edu.au (J.G. Sanjayan).

0958-9465/$ - see front matter © 2010 Elsevier Ltd. All rights reserved.
doi:10.1016/j.cemconcomp.2010.07.010

Table 1
Chemical composition of fly ash.

Chemical	Component (%)
Al_2O_3	30.5
SiO_2	48.3
CaO	2.8
Fe_2O_3	12.1
K_2O	0.4
MgO	1.2
Na_2O	0.2
SO_3	0.3
Loss on ignition	1.7

Sodium silicate solution (Na_2SiO_3) with specific gravity of 1.53 g/cc and sodium hydroxide (NaOH) flakes of 98% purity were supplied by PQ Australia. The chemical composition of the sodium silicate solution was Na_2O = 14.7%, SiO_2 = 29.4% and water = 55.9% by mass. Na_2SiO_3 and NaOH solutions were mixed one day prior to usage.

2.2. Specimen preparation

The geopolymer was synthesised from fly ash and a combination of sodium silicate solution and sodium hydroxide solution. The mixture of geopolymer was formulated with the molar oxide ratios SiO_2/Al_2O_3 = 3.21, Na_2O/Al_2O_3 = 0.41 and H_2O/Na_2O = 12.88. The materials were proportioned by weight and the mixing was conducted in a mechanical mixer of 20 l of capacity at 80 rpm for 5 min. Cylinder specimens were made for testing by using moulds of diameter 24 mm and length 48 mm. All the moulds were gradually filled and compacted in layers using vibration, and were sealed by plastic sheets. The covered moulds were cured in an oven at 60 °C for 18 h. After curing, specimens were de-moulded and kept in the laboratory until testing. In order to obtain smoother ends, the specimens were polished with a rock-grinder machine before testing. Specimens were tested at an age of 28 days.

2.3. Test apparatus

All the compressive strength tests were carried out on a closed-loop servo-control (500 kN) hydraulic pump actuator with a loading frame and an electric furnace. Fig. 1 shows the test apparatus (loading frame with furnace), while Fig. 2 shows the schematic diagram of the test set-up. The furnace, which contains a robust ceramic liner, provides heat uniformly around the specimen, since it is axis-symmetrical in design. The furnace has two 50 mm diameter openings, one at the top and one at the bottom, to allow high-temperature alloy loading rams to transmit compressive load from the test machine to the specimen being heated in the center of the furnace. The alloy loading rams were enclosed by ceramic tubes which protect the loading rams from direct thermal exposure. One concrete cylinder of 150 mm diameter and 150 mm height, made of high strength concrete, was placed on the top of the alloy loading ram as a heat insulator to protect the test machine from extreme temperature. The specimens were encased in a wire mesh, made of nickel-based alloy, to protect the interior of the furnace from explosion when specimens were crushed.

2.4. Heating and test procedure

Thermocouples were installed in two specimens in order to measure representative temperature. Two thermocouples were installed at mid-height of each specimen, one at the center and the other at the surface of the specimen. In the current investigation, the relatively small size (24 mm diameter) sample was used and

Fig. 1. Test equipment-loading frame with furnace.

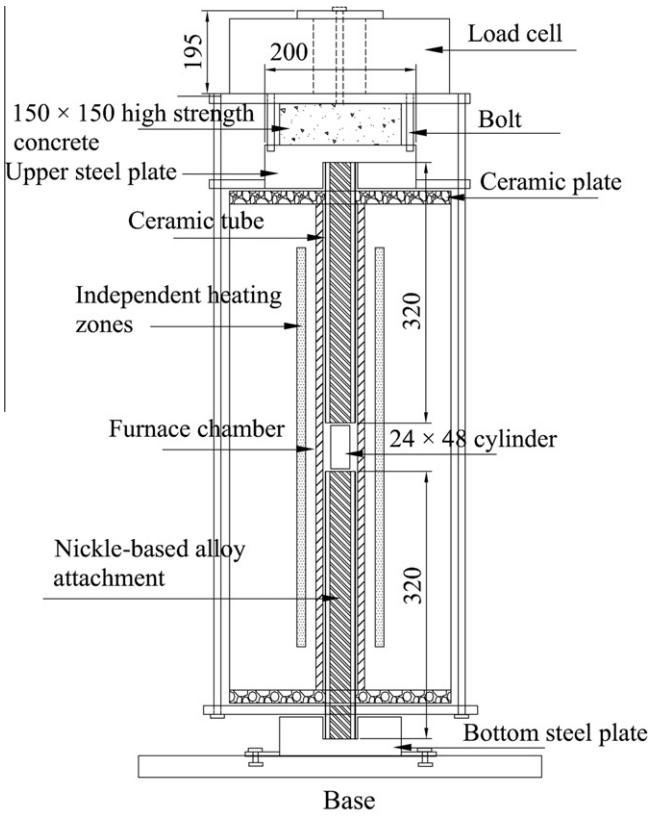

Fig. 2. Schematic of test set-up (all dimensions in mm).

a heating rate of 5 °C/min was adopted. This heating rate is consistent with RILEM 129-MHT [11] standard recommendation, where maximum heating rates of 0.5, 1, 2 and 4 °C were recommended for 150, 100, 75 and 50 mm diameter samples, respectively. The heating regime (Fig. 3) was as follows: the specimens were heated at 5 °C/min to their test temperatures; the temperature was then maintained for a period of 60 min, which in the preliminary test was found to be sufficient for reaching a nearly stable state within specimens. During the heating process, moisture in the specimens was allowed to escape freely. The specimens intended for residual strength testing were cooled by furnace cooling, i.e., left to cool with furnace switched off, until the samples reached room temperature.

A loading rate of 20 MPa/min was adopted for tests in this program which is consistent with the Australian standards and slightly lower than the 30 MPa/min proposed in RILEM 129-MHT [11] standards. It has been reported [12] that loading rate in the range of 6–600 MPa/min had no significant influence on compressive strength of cementitious materials.

In order to obtain data in the post failure region of the stress–strain curve, each specimen was also tested in a displacement control regime. At each temperature, the displacement rate was calculated based on the data taken from the test specimens that were crushed in load control regime. This displacement rate of geopolymer was altered by the increased plastic deformation as temperature increases, which was similar to that reported in Ordinary Portland Cement (OPC) concrete [13]. In the range of 23–520 °C, the displacement rate was 0.385 mm/min, and it was increased to 1.106 and 5.364 mm/min at 575 and 680 °C, respectively; therefore all specimens were loaded approximately at the rate of 20 MPa/min. The load and deformation of specimens were recorded continuously during each test.

A list of various tests carried out is presented below:

1. Reference strength test: the specimens were loaded to failure in both load and displacement control regime prior to heating.
2. Hot strength test: the specimens without being subjected to load were heated to the required temperatures and then loaded to failure while hot. Both load and displacement control regimes were applied during loading.
3. Stressed strength test: the specimens were first loaded in compression to a particular pre-determined load and then heated to the required temperatures. The load was then increased under a constant loading rate until failure occurred. Tests were performed at stress levels of $0.25\sigma_r$ and $0.50\sigma_r$, where σ_r is the reference strength at room temperature before heating.
4. Residual strength test: the specimens without being subjected to load were heated to the required temperatures and then allowed to cool within the furnace. The specimens were strength tested at room temperature. Both load and displacement control regimes were applied during strength tests. These tests were performed within two days of the tests of their companion in the hot strength tests as mentioned above in item (2).

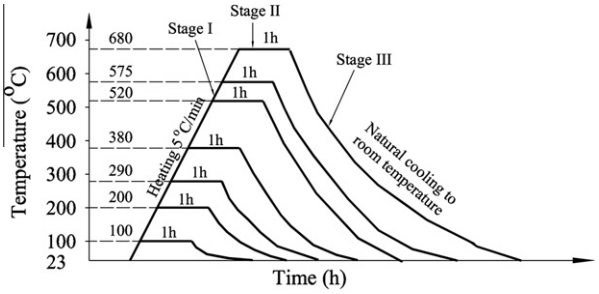

Fig. 3. Elevated temperature exposure regimes.

The TGA (Thermogravimetric Analysis) was conducted using a TG92-Setaram, with the temperature of the furnace programmed to rise at a constant heating rate of 5 °C/min up to 800 °C, under air flow.

The sorptivity test relies on a set-up where one face of the specimen is immersed to a depth of 1–2 mm and the water absorption by the specimen is monitored with time. The details of this test can be found in ASTM C1202-94. The results of the test provide a useful indication of the microcrack density of cementitious materials [14–16]. The specimens (before thermal exposure) used in sorptivity test were dried in an oven at 105 °C until there was no reduction in the specimen mass.

3. Results

3.1. Strain with temperature under constant load

The results of the strain of geopolymer specimens under different loads, as a function of temperature, are shown in Fig. 4. The strain curves show a region of very small expansion between 23 and 150 °C. It was followed by a small shrinkage from 150 to 290 °C. Then, a moderate level of expansion commenced at approximately 290 °C and continued until 520 °C. Above 520 °C, geopolymer specimens underwent significant contraction for the remainder of the temperature range up to 680 °C. With increasing stress levels, geopolymer specimens exhibited a tendency for an increase in compressive strain (contraction).

3.2. Strain with time under constant temperature and load

Fig. 5 shows change in strain (creep strain) with increasing time when the geopolymer specimens were subjected to constant load and temperature. In this case, the specimens were subjected to a constant stress/initial strength ratio of 0.25. It can be seen from the figure that geopolymer specimens exhibited expansion at 380 and 520 °C but shrinkage at 575 and 680 °C. The magnitude of strain was constantly increasing with increasing temperature; regardless of the strain direction (either expansion or contraction). Further the rate of change of the magnitude of strain decreased with time for each temperature (i.e. 380, 520, 575 and 680 °C). Half of the total strain measured typically occurred within the first 15 min of the monitored time (i.e. 1 h after the target temperature was attained). This is especially apparent in strain curve for 680 °C plotted within the figure.

Among observations presented above, two interesting behaviours could be further explored: (1) small expansion of geopolymer in the range of 380–520 °C; (2) significant contraction strain above 575 °C. Typically materials are expected to exhibit compressive strains under compressive stress. In contrast to this, the expansion value of loaded geopolymer increased with time and temperature.

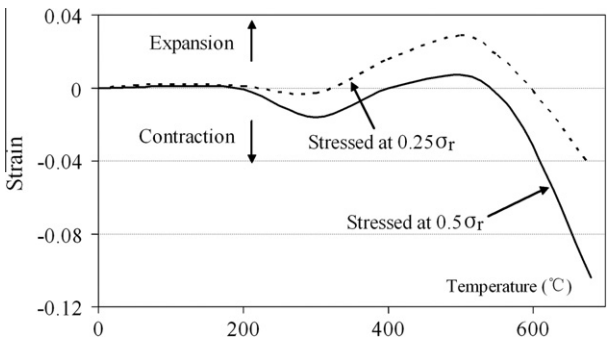

Fig. 4. Thermal strains under different stress levels, as a function of temperature.

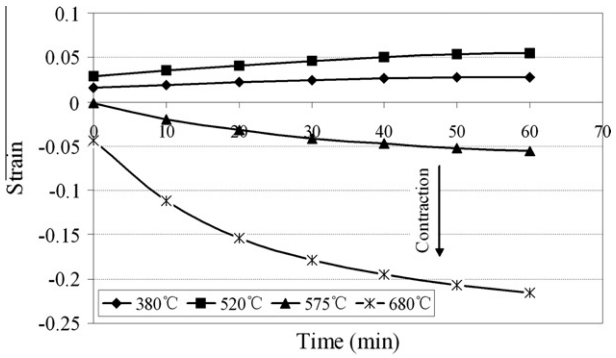

Fig. 5. Thermal strains as a function of time (for geopolymers stressed at $0.25\sigma_r$).

This may be as a result of stiffening effect in this range. This is further confirmed by the increase in hot strength of geopolymer in this temperature range, which will be discussed later.

Another interesting behaviour of Fig. 5 is the significant increase in compressive strain above 575 °C. The 1 h compressive strain increased from 0.05 to 0.22 over the small temperature range of 575–680 °C. At 680 °C, the large compressive strain in relatively short time clearly demonstrates a viscous-flow-type phenomenon which often occurs in glasses and metals at high temperatures. In both glasses and metals, this phenomenon is linked to the atomic or molecular self diffusion mechanism [17]. The structure of geopolymers has been proposed to be similar to that of aluminosilicate glasses [18,19]. Therefore, this mechanism may also be applicable to the large strain found in geopolymer in this temperature range.

3.3. Stress–strain relationship

The stress–strain curves for geopolymer specimens at elevated temperatures, tested in load and displacement control regime are shown in Figs. 6 and 7, respectively. Both figures show a similar tendency for the change in stress–strain curves with temperature. The strain corresponding to the peak strength did not significantly change up to about 520 °C. Above this temperature, the strains corresponding to the peak strength increased considerably, indicating a significant change in material behaviour. The peak strains (i.e. the strain corresponding to the peak strength) at 575 and 680 °C were respectively 20 and 140 times the peak strain attained at room temperature.

Over the investigated temperature range, the failure behaviour of geopolymer varied with temperature. Up to 575 °C, geopolymer specimens failed soon after reaching their peak strength which is

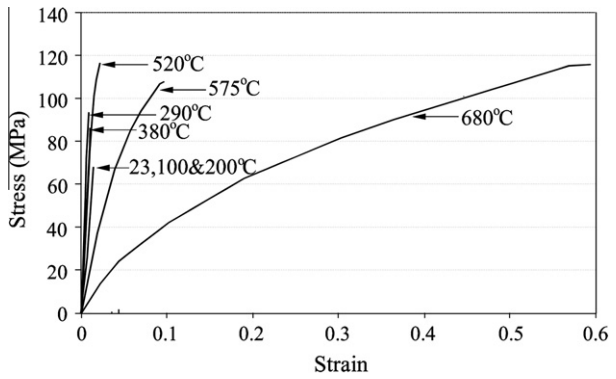

Fig. 6. Stress–strain curves for specimens at various temperatures (tested under load control).

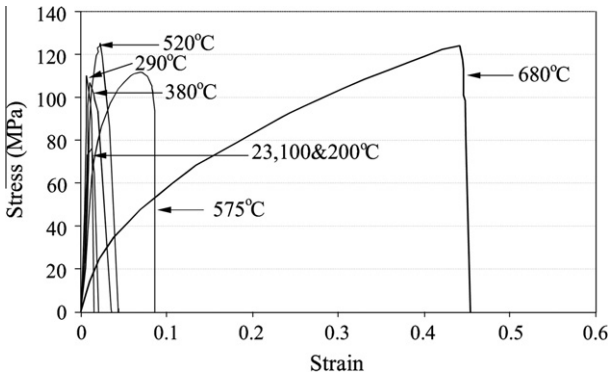

Fig. 7. Stress–strain curves for specimens at various temperatures (tested under displacement control).

evident when the stress–strain curves in Fig. 7 plunged vertically (post failure region). This shows that geopolymer specimens failed in a brittle nature. At 680 °C, the specimen sustained large deformation before fracture (Fig. 8), which indicates that geopolymer behaviour is viscoelastic nature at this temperature. However, as seen in Fig. 7, the geopolymer specimens at 680 °C still retained a brittle type of failure after reaching the peak stress. This failure was due to vertical crack as seen in Fig. 8.

3.4. Hot and residual compressive strengths

Fig. 9 shows the variation of hot and residual strength with temperature and the reference strength prior to heating. In the hot state, the strength measured in load control regime (σ_T^L) is similar to that measured in displacement control regime (σ_T^D). At each temperature, either σ_T^L deviation ($\sigma_T^L - (\sigma_T^L + \sigma_T^D)/2$) or σ_T^D deviation ($\sigma_T^D - (\sigma_T^L + \sigma_T^D)/2$) did not exceed 15% of their mean value ($(\sigma_T^L + \sigma_T^D)/2$). For the residual strength and reference strength, at least three specimens were used for each data and standard deviation was within 0.05.

In the range of 23–575 °C, the effects of temperature on the compressive strength (hot and residual) are given in Fig. 10. From 23 to 200 °C, there was no significant change in hot strength. From 200 to 290 °C, a remarkable increase in strength occurred; the increase was about 60% of the initial strength. In the range of 290–380 °C, geopolymers maintained their hot strength. The further temperature increase lead to a second increase in hot strength. The strength at 520 °C was about 179% of the initial strength. Then, the tendency that hot strength was higher than initial strength was maintained until 575 °C. The residual strength results (short dash

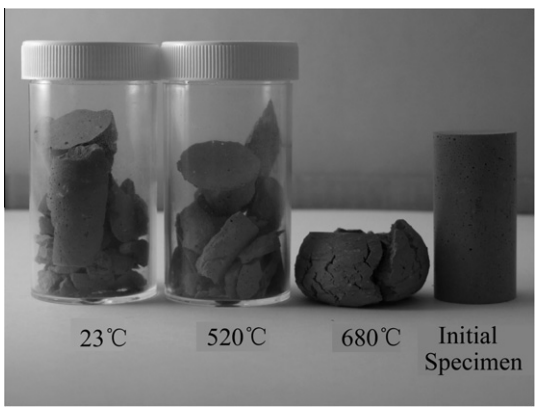

Fig. 8. The photograph of specimens after testing at various temperatures.

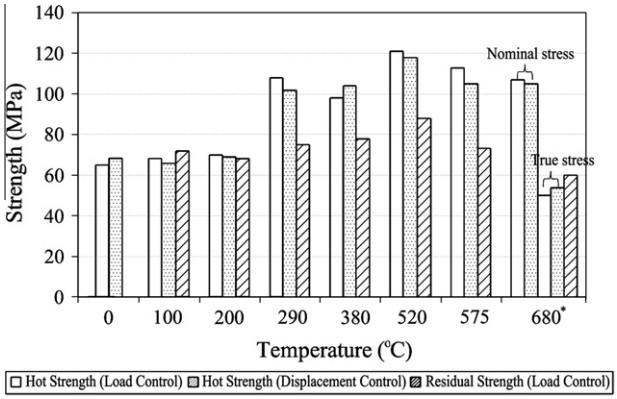

Fig. 9. Hot strength versus residual strength (*at 680 °C, true stress was obtained according to Eq. (1)).

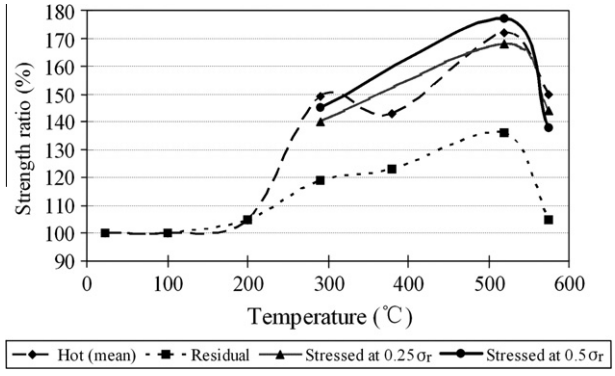

Fig. 10. Strength as a ratio of initial strength at various temperatures.

space line in Fig. 10) after heating show a trend similar to hot strength results (long dash space line). However, compared with the tests in a hot state, there was a loss of strength after cooling. The same figure also shows the effect of pre-load on hot strength. It seems that sustained pre-load did not produce significant effects on the strength of geopolymer specimens in the hot state. The strength in the hot state appeared to be only related to temperature but independent on pre-load.

At 680 °C, geopolymer specimens exhibited the large increase in the area of cross-section when they failed (Fig. 8). Therefore, the measured stress (nominal stress), defined as the load per unit original area of cross-section of specimen, can be significantly different from the true stress, which is the load divided by the current cross-section area. Generally, it is possible to correlate nominal and true value because the volume of material is constant in plastic deformation (rubbers, soft biological tissues, etc.). The relationship between nominal stress and true stress can be expressed as follows [17]:

$$\sigma_t = (1 - \varepsilon_n)\sigma_n \quad (1)$$

where σ_t is true stress, ε_n is nominal strain and σ_n is nominal stress. Both nominal stress (measured) and true stress (estimated by the above equation) are used for the strength of geopolymer at 680 °C.

It can be seen form Fig. 9 that a large drop in hot strength occurred at this temperature. The reason for this is that the large increase in cross-sectional area (Fig. 8) generated a decrease in stress. On the other hand, the test results of the residual strength after heating show that, compared with tests at 680 °C, there was a recovery of strength during cooling. This can be attributed to

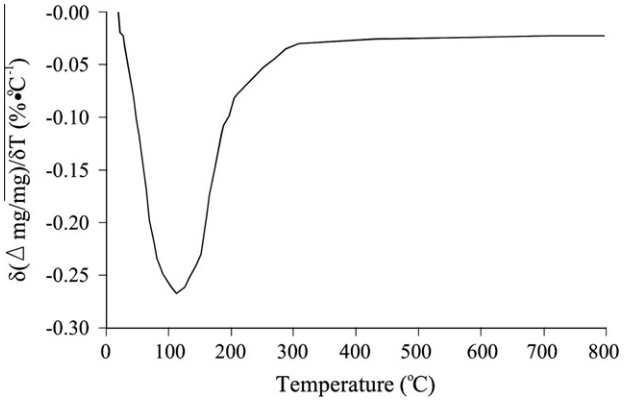

Fig. 11. Derivative thermogravimetric curve of geopolymer.

the fact that geopolymer specimens transited from viscoelastic nature to solid, when they cooled.

3.5. Thermogravimetric analysis

The derivative of the thermogravimetric (DTG) data is shown in Fig. 11. The rate of weight loss reached the maximum at around 100 °C and gradually slowed down until 300 °C. Between 300 and 800 °C, it was stable at a very low rate (close to zero). Similar to the authors' work, Kong et al. [7,8] found that the weight loss of geopolymer mainly occurred at temperatures below 300 °C. At around 100 °C, the DTG peak is attributed to the fast evaporation of free water. As most of the free water escaped at temperatures below 200 °C, the weight loss in the range between 200 and 300 °C is likely to be due to the loss of water liberated from further geopolymerisation process. The liberation of water during geopolymerisation has been reported previously [3].

4. Discussion

Geopolymer is an inorganic polymer which appears amorphous in X-ray diffraction analysis. Unlike in cement binder, where the main product of hydration is calcium silicate hydrate gel, which is the major provider of binder strength, in geopolymers, the main chemical process is geopolymerisation. From the chemical point of view, geopolymerisation is closely aligned with aluminosilicate gel formation [1]. The intrinsic difference in chemical structure of geopolymers and Portland cement (OPC) leads to their different behaviours at elevated temperatures. Two differences between geopolymers and OPC are significant. Firstly, it is believed that strains corresponding to peak load for OPC do not vary significantly between 100 and 550 °C [20]. The same is not true for geopolymer specimens. This is apparent in Fig. 12, where the strain corresponding to peak load for geopolymer specimens is plotted against temperatures; a large change in the strain started to occur when the temperature was beyond 520 °C. Secondly, OPC has a decreasing trend of hot strength in the range of 200–600 °C while geopolymer specimens exhibited a significant increase in hot strength in this range. These two distinct features of geopolymer specimens are further discussed in the following sections.

4.1. Glass transition temperature

One of distinct features is that geopolymer specimens exhibited abrupt transition behaviour at high temperature. In Fig. 8, the geopolymer specimens behaved as a rigid specimen and exhibited a brittle type of failure at temperatures less than 520 °C, while the geopolymer specimens sustained large extent of deformation

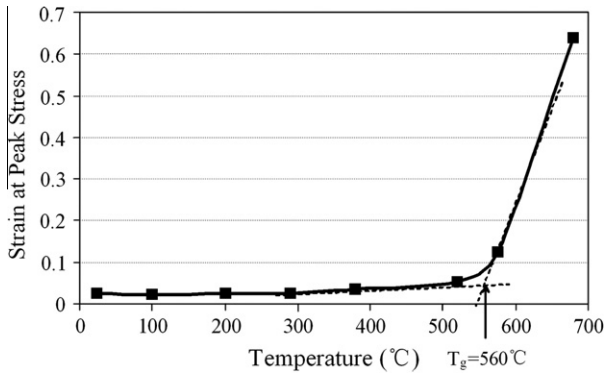

Fig. 12. Strain at peak stress versus temperature.

before failure at 680 °C, indicating that geopolymer specimen transit from a hard and relatively brittle condition to a viscous or rubbery one in this temperature range. This is a typical glass transition behaviour exhibited by some materials such as organic polymer materials [17], however, cementitious materials such as Portland cement based materials do not exhibit such behaviour. Therefore, geopolymer which is often benchmarked against Portland cement, this glass transition behaviour is of interest.

When the materials proceed through the temperature region associated with the glass transition, they exhibit a dramatic change in its slope of linear thermal deformation. Thus, the temperature that corresponds to the point of intersection of the slope of the deformation against temperature curve before and after the transition is generally assigned as the glass transition temperature, T_g. In Fig. 12, the intersection point of the slopes for these two extrapolations suggests that T_g of geopolymer was approximately 560 °C.

The important practical implication of the existence of T_g is that the structural usefulness of geopolymer concrete is limited to the temperatures below T_g. However, in structures exposed to high temperature, which occurs in connection with accidental fires, the high temperature beyond T_g is limited to exposed surface regions and the bulk of the geopolymer concrete may not reach this limit. Further, the T_g of polymers in general is strongly dependent on its chemical compositions [17]. It is thereby speculated that the T_g of geopolymer could also be tailored by appropriate raw material selection and mixture design. Further research in this area is needed.

4.2. Increase in hot strength

Another particular feature is that geopolymer specimens exhibited significant increase in strength at elevated temperatures. This trend is similar to those reported by previous investigations [6–10]. The previous researchers indicated that some geopolymer specimens increased in strength after exposure to 800 °C. However, actual temperature ranges where the strength increase occurred were not identified. Based on the results reported in this paper, the hot strength (thick dot line in Fig. 10) can be described as having a significant increase in value from 200 to around 290 °C, a level plateau thereafter, and a further increase from 380 to 520 °C.

The increase in strength of geopolymers is generally attributed to sintering process during heating. However, this mechanism may not be applied in the current investigation because the above two ranges are far below the sintering temperatures for geopolymers (700 °C) [21] and fly ash (1170 °C) [22]. When comparing hot strength results with the thermal deformation and weight loss results, it can be speculated that mechanisms for the strength increase in the two temperature ranges may be different because of the following reasons: Firstly, the geopolymer contracts in the range of 200–290 °C while it expands in the range of 380–520 °C. Secondly, the rate of weight loss in the lower temperature range is significantly higher than that in the higher temperature range.

Fig. 13 presents ΔT ($T_{surface} - T_{center}$) curve obtained in the transient state (stage I in Fig. 3). The ΔT value reached the maximum of 38 °C at about 200 °C. Beyond this temperature, a sharp drop in ΔT value was observed. This drop clearly indicates the release of heat within the specimens taking place in the range of 200–290 °C. Similar to our work, Rahier et al. [19] also found that the DSC (Differential Scanning Calorimetry) thermogram of geopolymer consists of a considerable peak in the exotherms in this temperature range. This peak is proven to be the characteristic of geopolymerisation [19]. Therefore, the strength increase in the range of 200–290 °C is attributed to the further geopolymerisation.

The strength increase in the range of 380–520 °C is less pronounced compared to that occurred in the range of 200–290 °C. The strength at 520 °C was 14% higher than that at 380 °C. It appears from literature that no distinguishable changes in this temperature range was observed by X-ray Diffraction (XRD) and Nuclear Magnetic-Resonance spectroscopy (NMR); nor were any significant thermic reactions detected by DSC (Differential Scanning Calorimetry) [18]. The small increase (up to 14%) in strength is attributed to the general stiffening of the geopolymer gel, or the increase in surface forces between gel particles due to the removal of absorbed moisture. It is noted that the latter reason is generally accepted for the strength increase occurred in cementitious materials at high temperatures [23,24].

4.3. Deterioration in strength during cooling

In the range of 290 to 575 °C, a notable decrease in strength during cooling process was observed in geopolymer specimens as

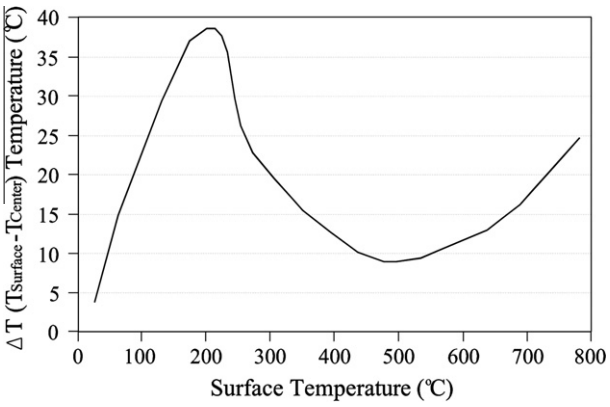

Fig. 13. ΔT curve of geopolymer in the transient state (stage I in Fig. 3).

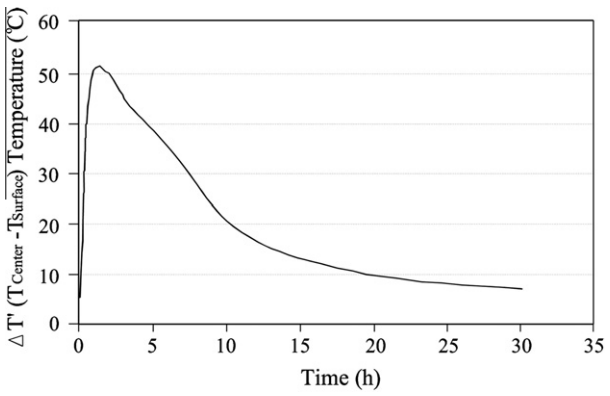

Fig. 14. $\Delta T'$ curve of geopolymer in the cooling process (stage III in Fig. 3).

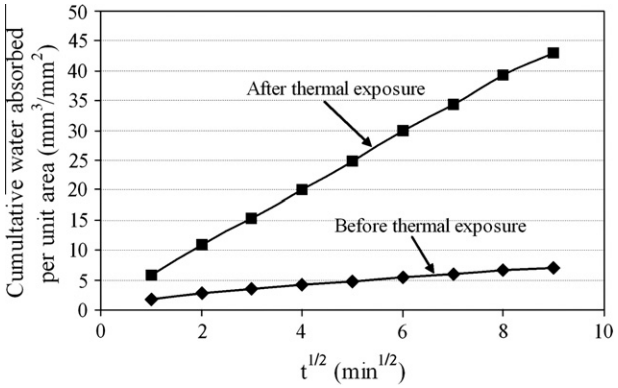

Fig. 15. Typical result of water absorption as a function of $t^{1/2}$.

shown in Fig. 10. After thermal exposure, the residual strength of geopolymer specimens degraded to 70% of the strength in the hot state.

Fig. 14 shows that the maximum ΔT ($T_{center} - T_{surface}$) value over a 12 mm length reached about 50 °C during cooling (stage III in Fig. 3). Kristensen and Hansen [25] experimentally demonstrated that temperature gradient required for cracking to occur in cement paste was between 20 and 30 °C over a 50 mm length. It is believed that the temperature gradient within geopolymer specimens is large enough to cause microcracking because: (1) the severity of thermal incompatibility (arising from temperature gradient) that geopolymer suffered in the current investigation is higher than the ones reported for Portland cement pastes [25]; (2) the ductility (i.e. the capacity to accommodate thermal incompatibility) of geopolymer is lower than that of Portland cement paste.

This is further supported by the results obtained in sorptivity test. The relationship between microcrack density and sorptivity has been extensively examined for cementitious materials [14–16]. In those studies, the researchers concluded that the presence of microcracks leads to significant increase of sorptivity. Fig. 15 shows that the measured sorptivity for geopolymer after thermal exposure was significantly higher than that of geopolymer before thermal exposure. The large increase in sorptivity is attributed to the fact that water may rapidly fill the microcracks due to the large capillary suction. Therefore, the strength loss during cooling is likely to be caused by thermal shock (i.e. cracking as a result of temperature gradient).

It should be noted that the test trends observed only for the geopolymer paste. For geopolymer concretes, aggregates will also have a major influence similar to the Portland cement concretes.

5. Conclusions

1. The geopolymer is found to exhibit glass transition behaviour at the temperature of 560 °C. This temperature was determined by monitoring the strains at peak stress at various temperatures. The strains at peak stress did not significantly change up to about 520 °C. Beyond glass transition temperature, these strains rapidly increased reaching as high as 0.64 at 680 °C, indicating significant change of material behaviour from solid to viscoelastic nature.
2. Two distinct behaviour patterns can be identified prior to reaching glass transition behaviour. In the temperature range from 200 to 290 °C, the geopolymer increased in strength while also undergoing significant contraction. This is attributed to the further geopolymerisation. In the range from 380 to 520 °C, a further strength increase was observed, but the geopolymer expanded at this time.
3. Sustained pre-load before heating appears to have no influence on the compressive strength of geopolymer specimens in a hot state. However, the increasing applied stress leads to high contraction at elevated temperatures.
4. Additional strength loss during the cooling suggests that geopolymer specimens are susceptible to damage resulting from thermal shock.
5. At any given test temperature, geopolymer specimens exhibited a nearly vertical descending branch of stress–strain curves after peak stress. This indicates that geopolymer specimens retained a brittle type of failure at all temperatures.

Acknowledgements

Authors gratefully acknowledge the financial support from the Australian Research Council Discovery Grant No. DP0664309 for this research work. Authors also gratefully acknowledge Professor Rangan's valuable comments and suggestions for this research work.

References

[1] Davidovits J. Geopolymers: inorganic polymeric new materials. J Therm Anal 1991;37(8):1633–56.
[2] Sumajouw DMJ, Hardjito D, Wallah SE, Rangan BV. Fly ash-based geopolymer concrete: study of slender reinforced columns. J Mater Sci 2007;42(9):3124–30.
[3] Rangan BV. Heat-cured, low-calcium, fly ash-based geopolymer concrete. Indian Concr J 2006;80(6):47–52.
[4] Hardjito D, Wallah SE, Sumajouw DMJ, Rangan BV. On the development of fly ash-based geopolymer concrete. ACI Mater J 2004;101(6):467–72.
[5] Duxson P, Provis JL, Lukey GC, Mallicoat SW, Kriven WM, van Deventer JSJ. Understanding the relationship between geopolymer composition, microstructure and mechanical properties. Colloids Surf A 2005;269:47–58.
[6] Kong D, Sanjayan JG. Damage behavior of geopolymer composites exposed to elevated temperatures. Cem Concr Compos 2008;30(10):986–91.
[7] Kong D, Sanjayan JG, Sagoe-Crentsil K. Factors affecting the performance of metakaolin geopolymers exposed to elevated temperatures. J Mater Sci 2008;43(3):824–31.
[8] Kong D, Sanjayan JG, Sagoe-Crentsil K. Comparative performance of geopolymers made with metakaolin and fly ash after exposure to elevated temperatures. Cem Concr Res 2007;37(12):1583–9.
[9] Pan Z, Sanjayan JG, Rangan BV. An investigation of the mechanisms for strength gain or loss of geopolymer mortar after exposure to elevated temperature. J Mater Sci 2009;44(7):1873–80.
[10] Dombrowski K, Buchwald A, Weil M. The influence of calcium content on the structure and thermal performance of fly ash based geopolymers. J Mater Sci 2007;42(3):3033–43.
[11] RILEM 129-MHT. Mechanical properties of concrete at high temperatures. Mater Struct 1995; 28: 410–14.
[12] Evans RH. Effect of rate of loading on some mechanical properties of concrete. In: Walton WH, editor. Mechanical properties of non-metallic brittle materials. London: Butterworths Scientific Publications; 1958. p. 175–92.
[13] Khoury GA, Grainger BN, Sullivan PJE. Transient thermal strain of concrete: literature review, conditions within specimen and behaviour of individual constituents. Mag Concr Res 1985;37(132):131–44.
[14] Collins F, Sanjayan JG. Microcracking and strength development of alkali activated slag concrete. Cem Concr Compos 2001;23(4):345–52.
[15] Sahmaran M, Li VC. Durability properties of micro-cracked on water absorption and sorptivity of ECC. Mater Struct 2009;42(5):593–603.
[16] Gagne R, Popic A, Pigeon M. Effect of water absorption on performance of concrete subjected to accelerated freezing and thawing tests. ACI Mater J 2003;100(4):286–93.
[17] Meyers M, Chawla K. Mechanical behavior of materials. New York: Cambridge; 2009.
[18] Barbosa VFF, MacKenzie KJD. Thermal behaviour of inorganic geopolymers and composites derived from sodium polysialate. Mater Res Bull 2003;38(2):319–31.
[19] Rahier H, Simons W, Mele BV, Biesemans M. Low-temperature synthesized aluminosilicate glasses: Part II. Rheological transformations during low-temperature cure and high-temperature properties of a model compound. J Mater Sci 1996;31(1):80–5.
[20] Dias WPS, Khoury GA, Sullivan PJE. Mechanical properties of hardened cement paste exposed to temperatures up to 700 C (1292 F). ACI Mater J 1990;87(2):160–6.
[21] Duxson P, Lukey GC, van Deventer JSJ. The thermal evolution of metakaolin geopolymers: Part 1 physical evolution. J Non-Cryst Solids 2006;352:5541–55.
[22] Erol M, Küçükbayrak S, Ersoy-Meriçboyu A. Characterization of sintered coal fly ashes. Fuel 2008;87(7):1334–40.

[23] Cheng FP, Kodur VKR, Wang TC. Stress–strain curves for high strength concrete at elevated temperatures. J Mater ASCE 2006;84(1):84–90.
[24] Lankard DR, Birkimer DL, Fondfriest FF, Synder MJ. Effects of moisture content on the structure properties of Portland cement concrete exposed to temperatures up to 500 F. Temperature and concrete, SP-25. Detroit: American Concrete Institute; 1971. p. 59–102.
[25] Kristensen L, Hansen TC. Cracks in concrete core due to fire or thermal heating shock. ACI Mater J 1994;91(5):453–9.